PERGAMON

Journal of Structural Geology 25 (2003) 389–408

JOURNAL OF STRUCTURAL GEOLOGY

www.elsevier.com/locate/jsg

Deformation and recrystallization of plagioclase along a temperature gradient: an example from the Bergell tonalite

Claudio L. Rosenberg[a,*], Holger Stünitz[b]

[a]*Freie Universität Berlin, Institut für Geologie, Malteserstr. 74-100 D-12249 Berlin, Germany*
[b]*Geologisches Institut, Bernoullistr. 32 CH-4056 Basel, Switzerland*

Received 22 January 2001; received in revised form 21 February 2002; accepted 27 February 2002

Abstract

Syn- to post-mylonitic tilting of the Bergell tonalite allows investigation of the deformation and recrystallization of plagioclase grains along a temperature gradient from the lower to the upper amphibolite facies. At the lowest temperatures recrystallization occurs by nucleation and growth of new grains having a different composition from the old grains. In contrast, at the highest temperatures recrystallization occurs by subgrain rotation associated with grain boundary migration. The temperature increase is inferred to induce this transition in two ways. First, at higher temperatures the anorthite content of the new grains is higher and thus the comositional difference between old and new grains is lower. Hence, the chemical driving potential is small compared with recrystallization at lower temperatures. Second, higher temperatures facilitate climb of dislocations and thus subgrain formation as well as grain boundary mobility. The temperature increase is also associated with a transition in the dominant deformation mechanism. Intracrystalline plasticity dominates deformation at lower temperatures, whereas at higher temperatures deformation occurs primarily by diffusion-accommodated grain boundary sliding, as indicated by the weakening of the indicatrix preferred orientation and the formation of a mixed plagioclase–biotite matrix with increasing deformation. Therefore, the strength of the mid to lower crust may be overestimated by dislocation creep flow laws for plagioclase. Lower crust rheology for polyphase rocks is better approximated by constitutive relationships involving diffusion accommodated grain boundary sliding.

Keywords: Plagioclase; Dynamic recrystallization; Grain boundary sliding; Nucleation and growth

1. Introduction

Models of crustal rheology commonly assume that the rheology of quartz controls the strength of the upper crust, and the rheology of feldspar controls the strength of the middle to lower crust (e.g. Ord and Hobbs, 1989). Mylonitic rocks containing interconnected quartz layers are widespread in upper to middle crustal mylonites, indicating that quartz indeed controls the rheology of these rocks. However, interconnected monomineralic layers or networks of feldspar in middle to deep crustal rocks are generally lacking. Investigations of high-temperature deformation of feldspar in amphibolite-facies and granulite-facies rocks show that feldspar is deformed viscously, but does not form monomineralic interconnected weak layers unless the modal abundance is very high, as in anorthosites (Ji et al., 1988; Ji and Mainprice 1990; Kruse and Stünitz 1999). Therefore, rheological data obtained from the experimental deformation of monomineralic feldspar aggregates might not be appropriate for modelling the rheology of the middle and lower crust.

Microstructures and recrystallization mechanisms of deformed plagioclase are often interpreted by comparing them with quartz microstructures (e.g. Lafrance et al., 1996). The latter study suggested that the recrystallization microstructures of plagioclase are produced by three temperature- and strain rate-dependent recrystallization mechanisms, similar to dynamic recrystallization in quartz (Hirth and Tullis, 1992). These mechanisms in plagioclase have been termed bulging recrystallization, rotation recrystallization, and high-temperature grain boundary migration recrystallization (Fitz Gerald and Stünitz, 1993).

There are several ways in which recrystallization of feldspar differs from that of quartz. Firstly, chemical disequilibrium may contribute to syndeformational recrystallization or even represent the main driving potential (e.g. chemically induced grain boundary migration = CIGM; Hay and Evans, 1987) for recrystallization of feldspar (Vernon,

* Corresponding author. Tel.: +49-30-838-70902; fax: +49-30-838-70734.
E-mail address: cla@zedat.fu-berlin.de (C.L. Rosenberg).

0191-8141/03/$ - see front matter © 2002 Published by Elsevier Science Ltd.
PII: S0191-8141(02)00036-6

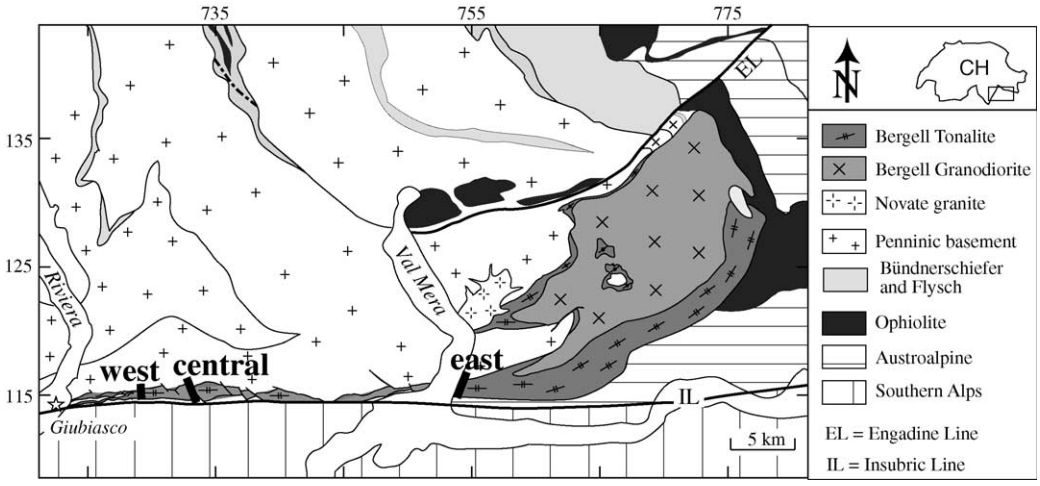

Fig. 1. Geologic map of the investigated area. The three studied cross-sections of the tail region of the Bergell Tonalite are indicated by the black bars and named West, Central, and East.

1975; White, 1975; Stünitz, 1998). Syndeformational recrystallization of feldspar has sometimes been interpreted as the result of nucleation and growth (Marshall et al., 1976) of feldspar grains with different composition (e.g. Sodre Borges and White, 1980) and many studies describe a compositional difference between old grains and dynamically recrystallized grains (Vernon, 1975; White, 1975; Brown et al., 1980; Brodie, 1981; Watts and Williams, 1983; Olesen, 1987; Yund and Tullis, 1991; Fitz Gerald and Stünitz, 1993; Molli 1994; Stünitz, 1998). Secondly, experimental deformation of fine-grained plagioclase aggregates has shown the occurrence of a transition from dislocation creep to diffusion creep induced by temperature, water activity, and strain rate (Tullis and Yund, 1991; Tullis et al., 1996). This result is in agreement with recent investigations of natural rocks, which suggest that plagioclase may deform by diffusion creep at amphibolite (Gower and Simpson, 1992; Selverstone, 1992) and granulite facies conditions (Martelat et al., 1999). This high-temperature diffusion creep regime is not known to occur in naturally deformed quartz aggregates.

We have studied the temperature-dependent transitions in microstructure, deformation processes and syndeformational recrystallization of plagioclase in the Bergell tonalite. Deformation of the Bergell tonalite occurs at amphibolite facies conditions along a temperature gradient, because tilting of the Bergell pluton resulted in the exposure of tonalitic mylonites that all have the same composition, and that have undergone the same deformation history, but under different temperature conditions and to different finite strain.

2. Geologic setting

The studied area is the 'tail' of the Bergell intrusion (Fig. 1), a steep tabular body of tonalite interpreted to be the feeder of the Bergell Pluton (Rosenberg et al., 1995). The tonalite tail is part of the Insubric Mylonitic Belt (e.g. Schmid et al., 1989) and the fabrics in these mylonites were formed during distributed ductile shearing with north-side-up displacements in a transpressive dextral shear regime (Heitzmann, 1987; Schmid et al., 1987, 1989). In the studied area, the Insubric Line is E–W striking and steeply N-dipping. It separates the Penninic nappes, which underwent amphibolite- to granulite-facies Tertiary metamorphism (North of the fault zone) from the Southern Alps, which were almost non-metamorphic during Tertiary time (South of the fault zone). As a consequence, vertical displacements in the order of 20 km are inferred for the Insubric Mylonitic Belt (Trümpy, 1980). The tonalite tail exhibits an E–W-striking and N-dipping foliation and steeply plunging stretching lineations, which vary in orientation from NE-plunging in the East to NW-plunging in the western part of the tonalite tail (see Berger et al. (1996) for discussion). The magmatic foliation and lineation have orientations parallel to the foliation and lineation produced by solid-state deformation, suggesting that the Insubric back-thrusting was both syn- and post-magmatic with respect to the intrusion of the Bergell tonalite (Rosenberg et al., 1995). Solid-state deformation occurred under amphibolite facies conditions. Later greenschist facies overprints are restricted to the dextral Riedel faults that dissect the tonalite tail (Fumasoli, 1974).

The inferred pressure during crystallization of the Bergell tonalite tail gradually increased from 600 MPa in the East to 850 MPa in the West (Reusser, 1987; Davidson et al., 1996). Nappe correlations (Trommsdorff and Nievergelt, 1983), geochronological dating (Villa and von Blankenburg, 1991) and paleomagnetic measurements (Rosenberg and Heller, 1997) confirm this westward pressure increase and indicate that it resulted from post-intrusive eastward tilting, which exposes increasingly deeper crustal levels from E to W. Hence, magmatic structures and mylonites were formed at increasingly higher temperatures and pressures towards

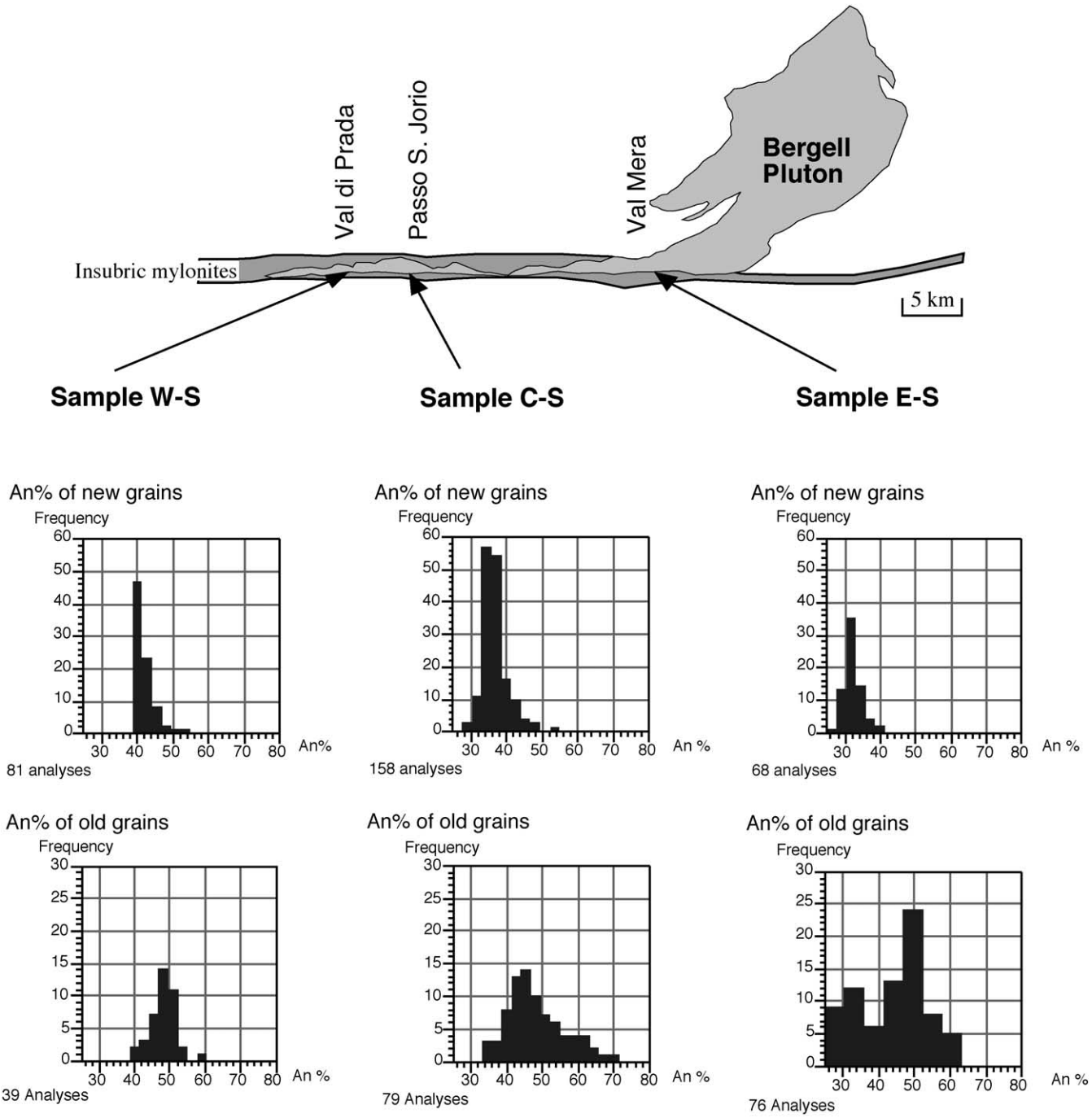

Fig. 2. Anorthite content of plagioclase in old and new grains of the high-strain samples of the tonalite tail (W–S, C–S and E–S). Each diagram represents cumulative data of several microstructural domains. Hence the compositional variation is greater than that of an individual microstructural domain, as illustrated in Figs. 6b and 10b. For chemical analyses see Rosenberg (1996).

the West (Rosenberg et al., 1994). The temperature gradient is documented by the progressively higher An-content of recrystallized plagioclase from E to W (Fig. 2) within the tonalite tail, which displays the same bulk chemical composition over its entire outcrop region (Reusser, 1987; Berger and Stünitz 1996). The estimated temperature range of deformation within the tonalite tail varies between 580 and 670 °C, based on mineral parageneses (Berger et al., 1996). The retrograde metamorphic reaction that takes place during deformation of plagioclase is:

$$\text{Hornblende} + \text{K} - \text{feldspar} + \text{Anorthite} + \text{Biotite1} + \text{Magnetite} + \text{H}_2\text{O} \Rightarrow \text{Epidote} + \text{Biotite2} + \text{Albite} + \text{quartz}$$

In addition to the E–W temperature gradient, the tonalite tail exhibits a N–S strain gradient across the Insubric fault

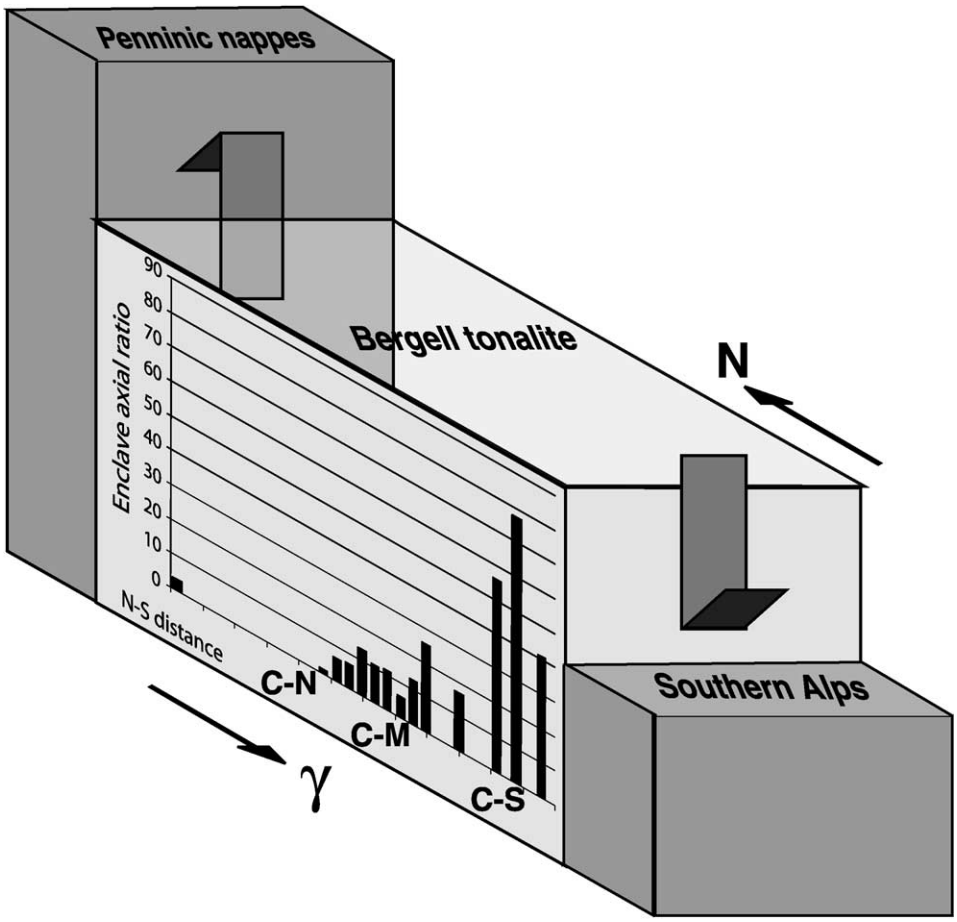

Fig. 3. Schematic block diagram, showing the southward increase in the axial ratio of mafic enclaves in the Central profile. Each bar indicates the average axial ratio of mafic enclaves measured on one outcrop, on the *XZ* plane. Total number of enclaves measured: 62. These measurements and the southward increase in strain are consistent with previous studies (Vogler and Voll, 1981; Fisch, 1989; Berger et al., 1996).

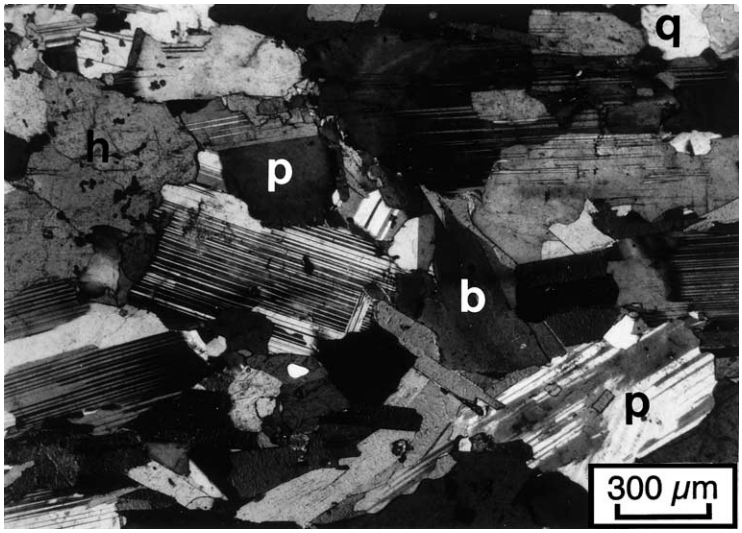

Fig. 4. Microphotograph of magmatically foliated Bergell tonalite. Note the shape preferred orientation of plagioclase grains and the lack of internal deformation of magmatic grains. b: biotite; h: hornblende, p: plagioclase; q: quartz.

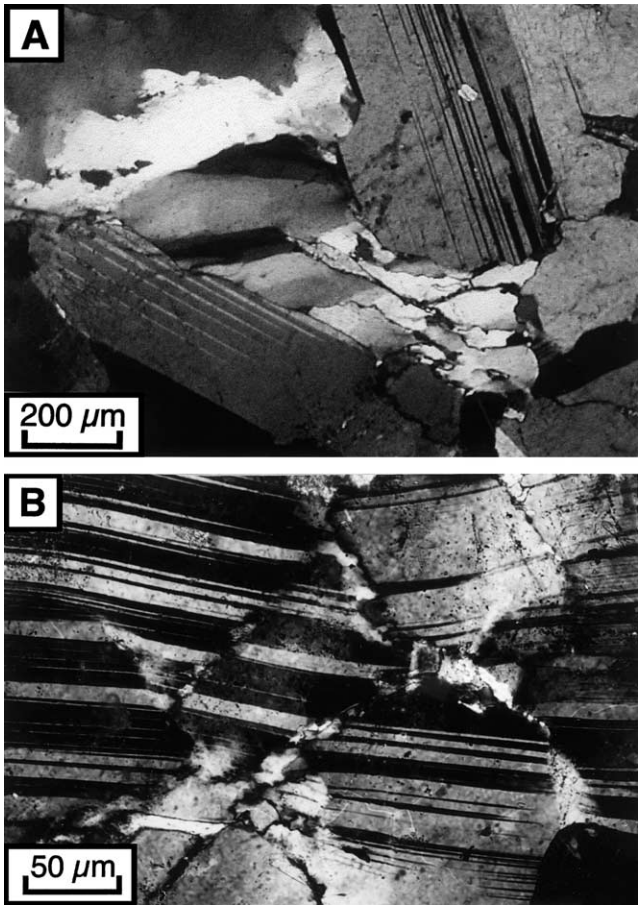

Fig. 5. Low T, low strain sample (E–N). (A) Micrograph with crossed polarizers, showing euhedral grains of plagioclase wrapped around by dynamically recrytallized and plastically deformed quartz. (B) Micrograph with crossed polarizers, showing conjugate sets of fractures within a plagioclase grain.

zone (Vogler and Voll, 1976, 1981; Fisch, 1989; Berger et al., 1996). Strain gradually increases from N to S, i.e. towards the contact with the Southern Alps (Fig. 3). The relative increase in strain was estimated by measuring the axial ratios of magmatic enclaves. There is no field evidence for a competence contrast between enclaves and tonalite, suggesting that enclaves recorded a similar strain intensity as the tonalite. Part of this strain affected the enclaves and the tonalite in the magmatic state.

3. Microstructures

For the sake of clarity, samples in this study are labelled in relation to their geographic position within the tonalite tail (Fig. 1). The first letter indicates the cross-section from which the sample is taken (W for the Western, C for the Central, and E for the Eastern cross-section), corresponding to the relative temperature conditions of deformation and recrystallization. The subsequent letter indicates the position of the sample within each N–S cross-section and therefore the relative strain intensity (N for North, M for Middle, and S for South).

3.1. Protolith

The protolith of the solid-state deformed tonalites exhibits a magmatic foliation, i.e. a shape preferred orientation (SPO) of largely euhedral plagioclase and hornblende grains; Plagioclase grains form a continuous framework. There is no evidence for crystal plastic deformation except for local and weak bending of some grains (Fig. 4). The magmatic grains of plagioclase are tabular parallel to (010) and elongate parallel to [100]. Plagioclase grains are up to 2 mm long (longest axis of the plagioclase lath), but some smaller grains of plagioclase also occur in finer-grained portions of the tonalite matrix.

3.2. Eastern cross-section (lowest solid state deformation temperature)

At low strain (samples E–N and E–M), the euhedral shape of plagioclase phenocrysts is largely preserved. Most of the strain is accommodated by crystal plastic deformation of biotite and quartz, which together form interconnected weak layers, wrapping around the plagioclase grains (Fig. 5a). Locally, plastic deformation of plagioclase occurs (bending of the twin planes and undulatory extinction), but there is no evidence for dynamic recrystallization or neocrystallization, i.e. nucleation and growth of new grains of different composition. Grain size reduction of plagioclase is very limited and is caused by fracturing (Fig. 5b).

At high strain (sample E–S), plagioclase porphyroclasts exhibit some internal deformation structures (bending of the twin planes, deformation twins, undulatory extinction). In some cases, a part of the old clast is bent, and the region of maximum bending can be followed into a fracture, similar to microstructures in Fig. 5b, suggesting that fracturing is accompanied by crystal plastic deformation. Thus, micromechanisms of deformation could be transitional between frictional and plastic, although an entirely brittle nature of the 'bending' on the sub-light-microscopic scale cannot be excluded on the basis of light microscope observations (Tullis and Yund, 1987).

In the high strain sample plagioclase do recrystallize and 20% of the total volume of plagioclase consists of new grains, with average longest axis of 120 μm. New grains develop predominantly at the boundaries of the old magmatic plagioclase porphyroclasts, forming core and mantle structures (Fig. 6a). The anorthite content of the new grains differs from that of the old grains (Fig. 2). Old grains are zoned with an anorthite content of approximately 30–35% at the rims (Fig. 2) and up to 65% (Figs. 2 and 6b) within the core. New grains have a mean anorthite content of 31%, but their composition ranges from 25 to 40% An (Figs. 2 and 6b). It should be noted that the compositional ranges of Fig. 2 represent compilations of several microstructural domains and thus are larger than compositional

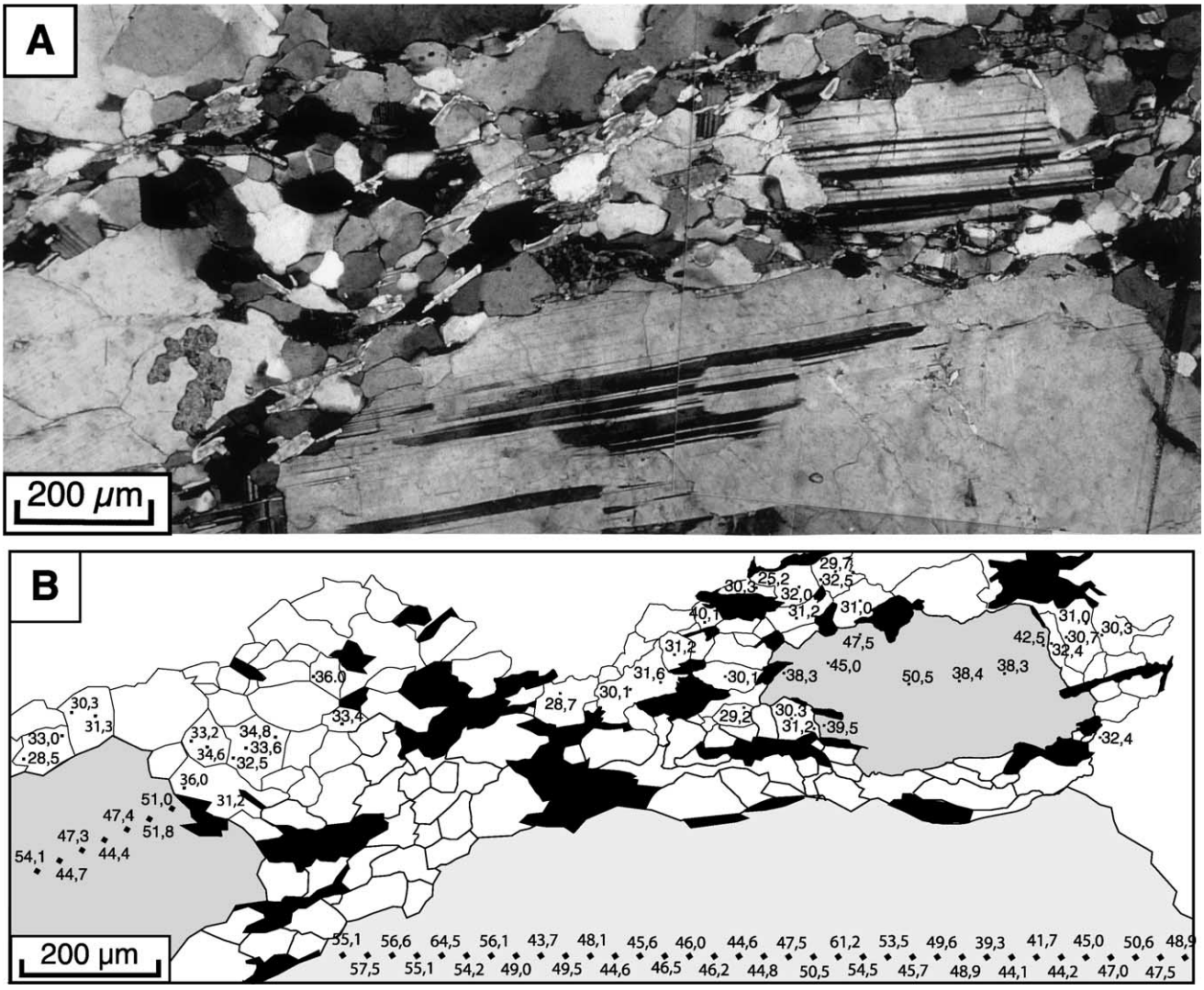

Fig. 6. Low T, high strain sample (E–S). (a) Micrograph with crossed polarizers, showing core and mantle structures in plagioclase. Note the weak bending of twin planes and the undulose extinction of the old grains, but the lack of polygonized subgrains. (b) Line drawing of the boxed portion of (a), showing the spatial distribution of the An component in plagioclase of the cores and mantles. Shaded are as indicate the old grains. Black grains are biotites.

ranges of individual microstructural domains (e.g. Fig. 6b). The anorthite content of the new grains is relatively constant throughout the recrystallized mantle region (Fig. 6b) and the boundary between old and new grains coincides with a sharp increase of anorthite content. Hence, it is not likely that the compositional difference between old and new grains reflects pre-existing differences in composition due to zonation of the phenocrysts; it is more likely the result of neocrystallization. Furthermore, the boundary between the recrystallized mantle area and the core (porphyroclast) is sharp (Fig. 6a), lacking the intermediate zone of subgrains that is typically found in core and mantle structures of quartz (White, 1976). Subgrains are never observed in the light microscope. The absence of subgrains and the systematic sharp compositional difference between old and new grains indicate that the core and mantle structures were not formed by progressive subgrain rotation recrystallization (Hobbs, 1968; Guillopé and Poirier, 1979). Syndeformational recrystallization of the new grains is probably not predominantly driven by strain energy (i.e. a recovery process), but appears to be largely driven by compositional disequilibrium.

Within the aggregates of new plagioclase grains, some biotite grains also occur (Fig. 6b). They are fine-grained and oriented approximately parallel to the foliation. Since the phenocrysts of plagioclase never have any biotite inclusions, the occurrence of biotites between the new grains of plagioclase cannot be explained as a primary magmatic feature. The systematic occurrence of biotite within these aggregates indicates either mechanical mixing or nucleation of new biotite between plagioclase grains during deformation. Mechanical mixing is unlikely because the aspect ratio of domains of mixtures of biotite and plagioclase grains is low (Fig. 7), suggesting that they did not deform to large strains. The dispersed biotite and plagioclase aggregates probably result from nucleation and growth of new phases during deformation according to the reaction given above.

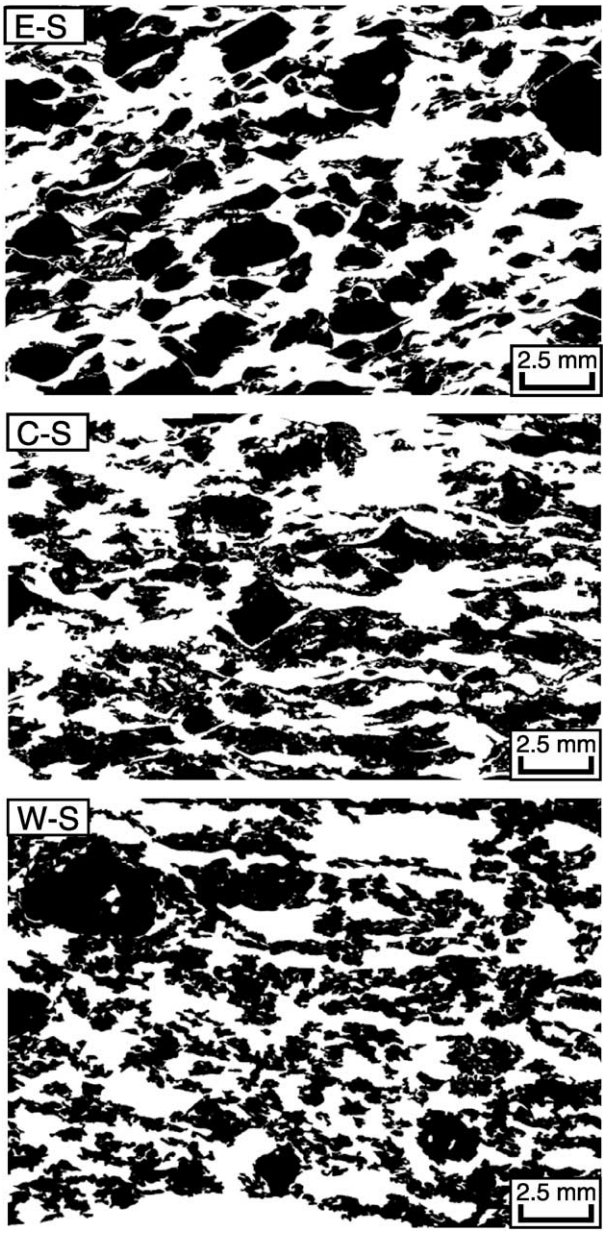

Fig. 7. Line drawings of thin sections illustrating the spatial distribution of plagioclase in high strain samples E–S, C–S and W–S. Plagioclase in sample E–S occurs predominantly as porphyroclasts. In contrast, in sample W–S porphyroclasts are rare and most plagioclase occurs as recrystallized grains homogeneously distributed in the polymineralic matrix.

3.3. Central cross-section (intermediate solid state temperature conditions)

At low strain (C–N), plagioclase porphyroclasts are large (up to 3 mm) and euhedral shapes are rarely preserved because of abundant lobate grain boundaries. Fig. 8 shows an example of a lobate contact between two neighbouring plagioclase grains and the distribution of anorthite content within both grains. No significant compositional variation is observed across the grain boundaries; the compositional variation within grains is greater than the difference across grain boundaries. Therefore, the migration of the boundary between grains is probably not controlled by a chemical driving potential. Since the grain boundary geometry does not represent an equilibrium configuration, it is likely that the geometry results from migration processes due to a mechanical driving potential (strain energy). The large penetration of one grain into another suggests a high local boundary mobility. This interpretation is further supported by the fact that the majority of magmatic phenocrysts has been destroyed by grain-boundary migration, despite the low strain acquired by this sample. No evidence for fracturing is observed, in contrast to the low strain sample of the Eastern cross-section (E–N).

Intracrystalline plasticity of the plagioclase grains in the form of spatially distributed bending of the entire lath is common. In some cases the area of maximum bending of the plagioclase lath is localized and forms a grain boundary with a small misorientation. Such a boundary can be continuously followed into a sharp and lobate grain boundary with a large misorientation (Fig. 9a and b), indicating the migration of a grain boundary which originally formed by subgrain rotation. The distribution of the anorthite content around such a migrated low angle boundary is unsystematically distributed in neighbouring grains (Fig. 9b). Therefore, grain boundary migration did not involve a chemical change.

At higher strain (C–M and C–S), new grains of plagioclase of different composition (Fig. 10b) and strongly reduced size develop adjacent to the old grains (Fig. 10a). In sample C–S, 59% of the total amount of plagioclase has recrystallized. The increase in the volume fraction of recrystallized grains compared with sample E–S (lower temperature) occurs together with an increasing dispersion of the new grains with other phases (Fig. 7). The new grains are mostly distributed within the tails of porphyroclasts, or within completely recrystallized elongate lenses of plagioclase aggregates (Fig. 11). Core and mantle structures exist, but they are less common compared with the lower temperature sample E–S. The average grain size of the new grains (average longest axis is 330 μm) is larger than that in the high strain samples of the lower temperature cross-section. The boundary between new grains and old grains is sharp and often coincides with a marked change of plagioclase composition (Fig. 10b). However, some optical-scale subgrains can be observed at the margins of the old grains. Their size is generally smaller than that of the new grains, suggesting that some grain boundary migration occurred. The anorthite content of most new grains in sample C–M varies between 32 and 38% (Figs. 2 and 10b). The old grains exhibit a normal zonation ranging from An 55–60% in the core to An 34–50% at the rims (Fig. 10b). The smaller compositional difference between old and new grains compared with the lower temperature Eastern cross-section is due to a higher An-content of the new grains (Fig. 2). The range of compositional variation of new grains is always more restricted than that of the old clasts. Pure monomineralic

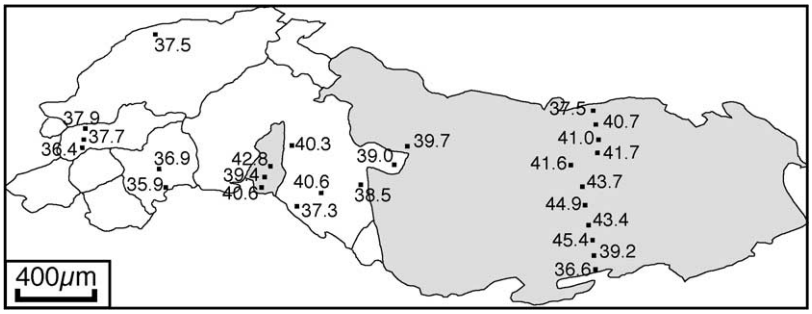

Fig. 8. Line drawing of a part of the intermediate T, low strain sample C–N, showing the spatial distribution of the An component of the plagioclase grains. Shaded grains have the same extinction angle under the light-microscope. It is therefore suggested that they may form a single grain that is dissected in the plane of the present thin section.

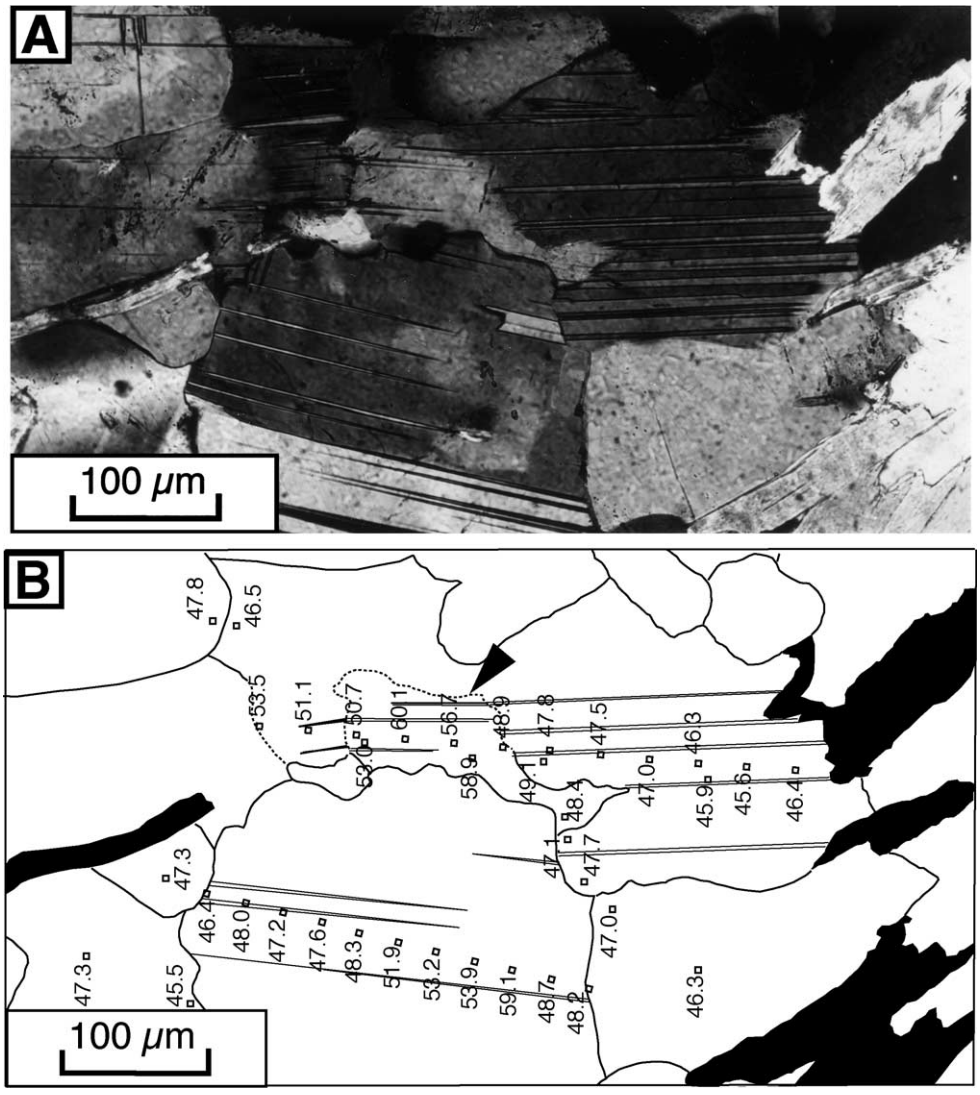

Fig. 9. Intermediate T, low strain sample C–N. (A) Micrograph with crossed polarizers, showing a lobate (migrated) grain boundary passing into a lobate (migrated) subgrain boundary. Arrowhead indicates the continuous, but deflected twin plane across a subgrain boundary. (B) Line drawing of Fig. 8a, showing the spatial distribution of the An component of the plagioclase grains. Dotted line: subgrain boundary. Continuous line: grain boundary. Black grains: biotites.

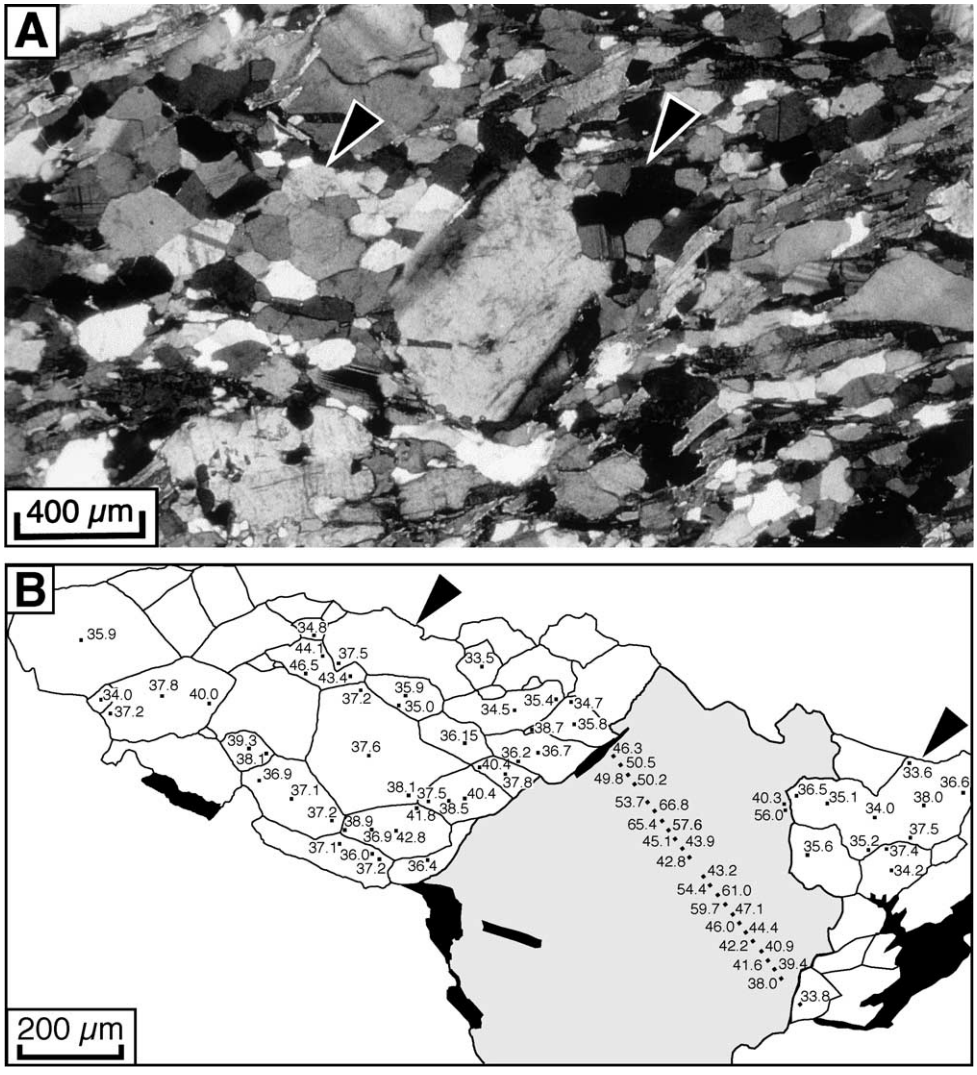

Fig. 10. Intermediate T, high strain sample C–S. (A) Micrograph with crossed polarizers showing recrystallized grains of plagioclase in the pressure shadow of a plagioclase clast. (B) Line drawing of the central part of Fig. 10A, showing the spatial distribution of the An content of the plagioclase grains. Small grains are new grains which appear to have resulted from subgrain rotation and grain boundary migration. There is a compositional difference between old and new grains. Shaded area indicates the old grain. Biotite grains are shown in black. Arrow heads point to the same new grains in Figs. 10A and 10B.

aggregates of new plagioclase grains are rare; as in sample E–S, some biotite is present in plagioclase aggregates (Fig. 10a).

3.4. Western cross-section (highest solid state deformation temperature)

In the lowest-strain sample (W–N) magmatic euhedral shapes are nearly absent due to lobate grain boundaries, but grain sizes are large (longest axes are 2 mm long), suggesting that the old magmatic grain boundaries have migrated extensively. Large scale (up to 300 μm) migration of grain boundaries is common in this sample. Interphase boundaries of plagioclase and quartz are strongly lobate (Fig. 12). The euhedral shapes of plagioclase in the magmatic protolith indicate that the lobate interphase boundaries result from deformation and/or chemical exchange and transport during syndeformational metamorphism. The chemical reaction responsible for the change in plagioclase composition (see above) produces quartz, and possibly some of the quartz precipitates at the boundaries of plagioclase. Plagioclase and quartz grain shapes do not differ systematically, indicating no obvious competence contrast between these two phases during solid state deformation. This situation is in contrast to the low strain and lower temperature sample (E–N), where quartz deforms plastically and aggregates of quartz wrap around more competent plagioclase grains (Fig. 5a). We therefore suggest that diffusive processes (dissolution and reprecipitation) at interphase boundaries accommodate part of the deformation at the highest temperatures (≤670 °C). Cuspate boundaries between quartz and feldspar in gneisses deformed in the absence of melt at high-temperature (≥650–750 °C) have previously been interpreted as the

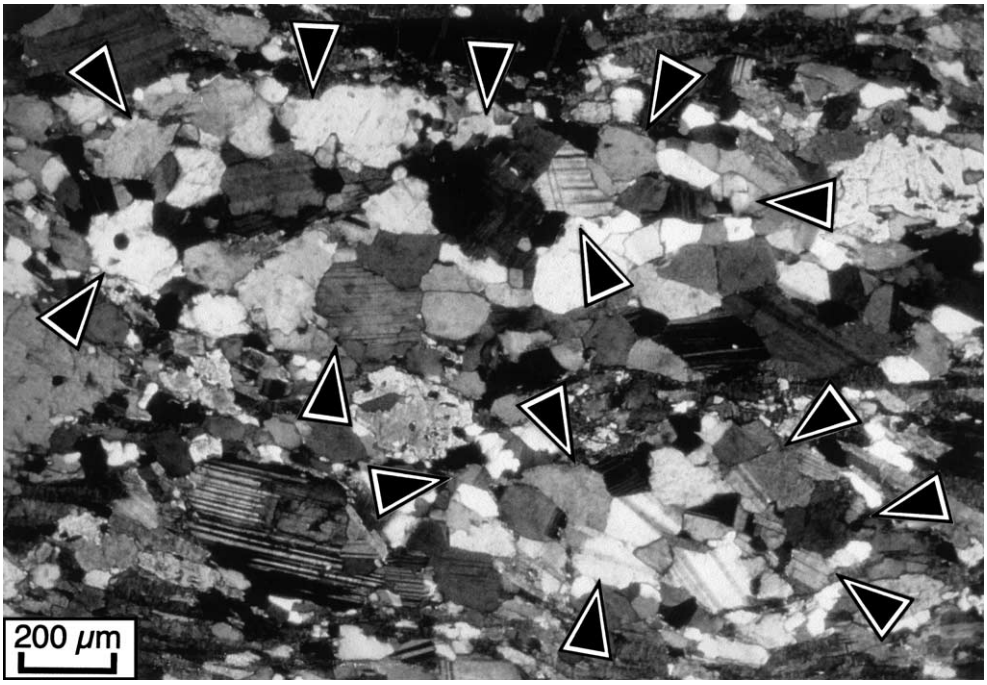

Fig. 11. Intermediate T, high strain sample C–S. Photomicrograph with crossed polarizers of two monophase plagioclase lenses entirely recrystallized. Arrow heads delineate the outline of plagioclase lenses.

result of diffusion creep (Gower and Simpson, 1992) in amphibolite facies granodioritic gneisses, and by Martelat et al. (1999) in granulite-facies rocks.

At higher strain (W–M), a grain size reduction and a higher aspect ratio of the plagioclase aggregates is observed. Elongate lenses of plagioclase aggregates consist of large grains (average long axis of 700–800 μm) with lobate grain boundaries. The migration of grain boundaries formed by progressive subgrain rotation is inferred from the commonly observed presence of weakly rotated subgrains at the margins of the old grains and by the lobate shape of many boundaries of small grains adjacent to porphyroclasts. Some

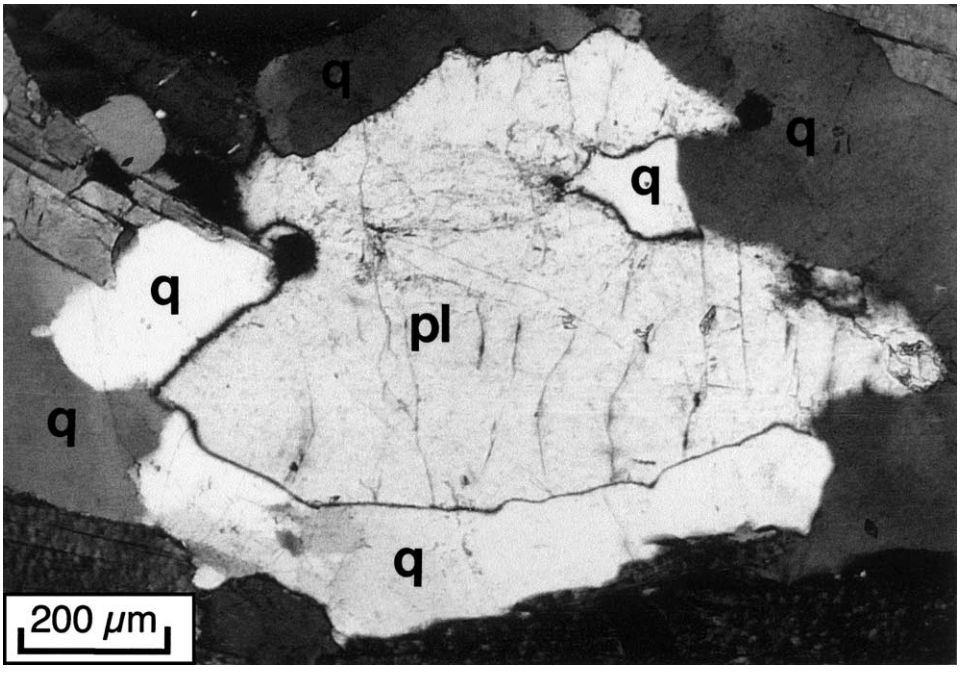

Fig. 12. High T, low strain sample W–N. Photomicrograph with crossed polarizers of a plagioclase grain (pl), partly replaced by quartz (q), showing lobate quartz and plagioclase boundaries, which are common for samples deformed at high temperatures.

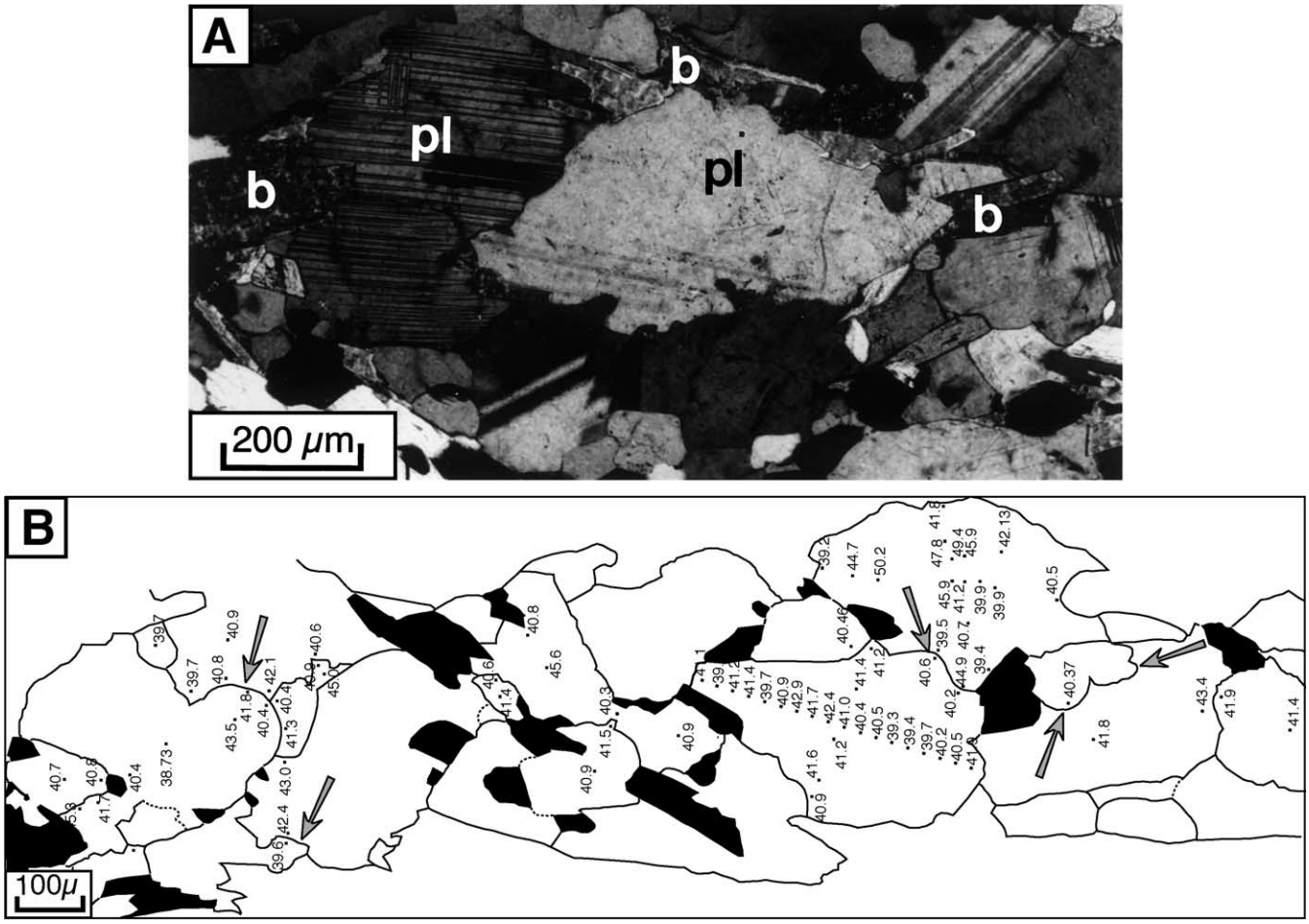

Fig. 13. High T, high strain sample W–S. (A) Microphotograph with crossed polarizers illustrating the plagioclase (pl)–biotite (b) matrix. Note the lobate grain boundaries of plagioclase and the dispersed distribution of biotite and plagioclase. (B) Line drawing, showing the spatial distribution of the An content of the plagioclase new grains. Note the small range of variation in the An content and the lack of compositional changes across lobate grain boundaries (indicated by arrows). Black grains are biotites.

low angle grain boundaries can be continuously followed into high angle lobate grain boundaries, as previously described and illustrated in Fig. 9a and b. No core and mantle structures developed (Fig. 13a and b).

At the highest strain (W–S), 81% of the total volume of plagioclase has recrystallized. The distribution of the recrystallized grains is more dispersed with other phases than that of the moderate temperature sample C–S (Fig. 7). The new grains have a large grain size (average longest axis 370 μm) and are generally twinned. The anorthite content of these grains is slightly lower than that of the old grains (Figs. 2 and 13b), but the compositional difference between old and new grains is much smaller than that in both the lower temperature cross-sections further East (Fig. 2). The compositional variation of the anorthite content across a migrated (lobate) grain boundary (see full arrows in Fig. 13b) is smaller than the compositional variation within individual grains. Therefore, migration of the grain boundary is probably not compositionally induced.

Compared with both cross-sections further East, more biotite is present within the plagioclase recrystallized aggregates of this specimen. In fact, new plagioclase grains are part of a biotite–plagioclase composite matrix, rather than a plagioclase aggregate. In contrast to the low temperature, high strain sample E–S, biotite grains locally transect plagioclase–plagioclase contacts (Fig. 13) and they are partly enclosed within the plagioclase grains. This suggests nucleation and growth of biotite or plagioclase grains and/or extensive grain boundary migration of plagioclase.

4. Indicatrix preferred orientation (IPO)

We measured the indicatrix preferred orientation (IPO) of the protolith and the high strain samples using a U-stage microscope. By comparing the IPO of the solid state deformed samples with that of the protolith, it is possible to infer differences in the deformation processes between samples. The orientation of the optical axes of plagioclase forms small angles to the crystallographic axes in the compositional range of the new grains of our samples (e.g. Burri et al., 1967). $n-\gamma$ makes an angle of 8–22°

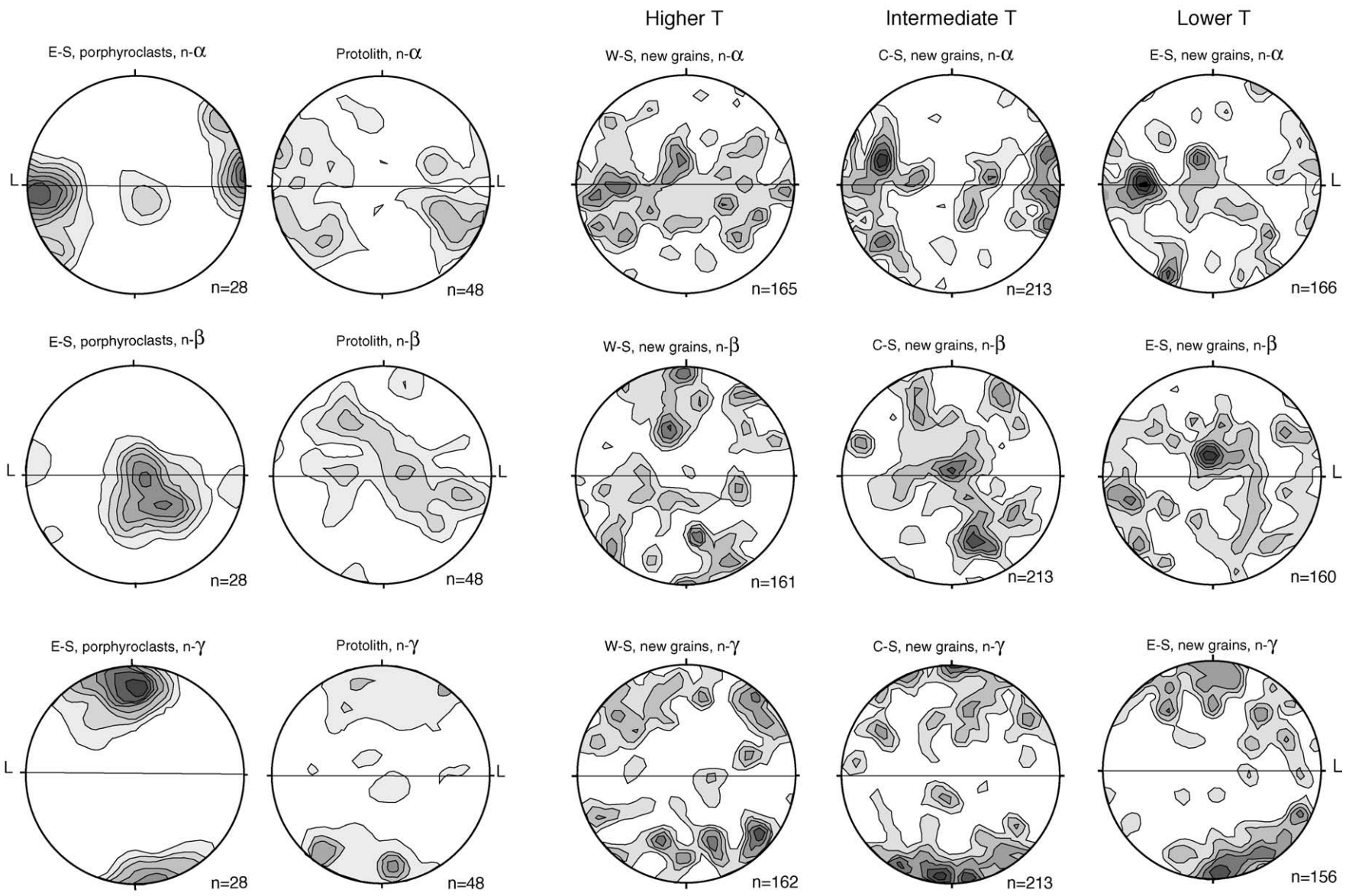
A: Old grains
B: New grains, high-strain samples
Higher T
Intermediate T
Lower T
E-S, porphyroclasts, n-α
Protolith, n-α
W-S, new grains, n-α
C-S, new grains, n-α
E-S, new grains, n-α
E-S, porphyroclasts, n-β
Protolith, n-β
W-S, new grains, n-β
C-S, new grains, n-β
E-S, new grains, n-β
E-S, porphyroclasts, n-γ
Protolith, n-γ
W-S, new grains, n-γ
C-S, new grains, n-γ
E-S, new grains, n-γ
L
n=28
n=48
n=165
n=213
n=166
n=161
n=213
n=160
n=162
n=213
n=156

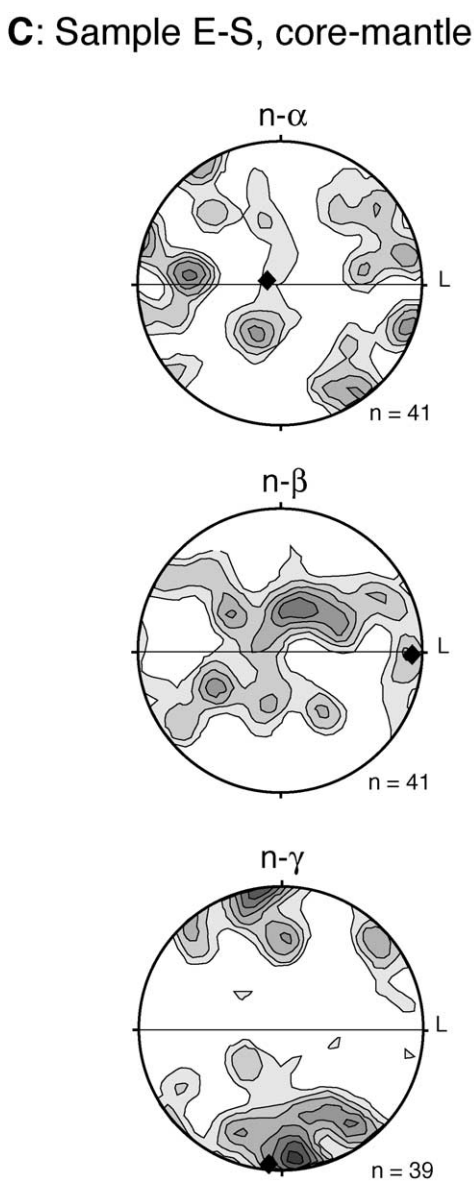

Fig. 14. (*continued*)

with the normal to the (010)-plane of plagioclase, $n-\alpha$ makes an angle of 2–12° with [100], and $n-\beta$ makes an angle of 11–28° with the normal to (001).

4.1. Protolith and porphyroclasts

The $n-\gamma$ direction of the phenocrysts in the magmatically foliated protolith (Fig. 14a) is oriented normal to the foliation plane, indicating that the (010) plane is parallel to the foliation. Both $n-\alpha$ and $n-\beta$ are close to the foliation plane, and the maxima of $n-\alpha$ are located close to the lineation. The IPO pattern of plagioclase porphyroclasts in sample E–S is similar to that of the magmatic phenocrysts of the protolith (Fig. 14a), but the IPO maxima of the porphyroclasts in the solid state deformed rock are approximately twice as strong as those of the phenocrysts in the magmatic protolith. This initial plagioclase fabric is the result of rigid particle rotation of phenocrysts (displaying a tabular shape anisotropy with $n-\alpha$ close to the long axis and $n\gamma$ normal to the largest flat surface of grains) in a crystallizing and deforming melt + crystal mixture. The porphyroclasts exhibit the same euhedral shape as the phenocrysts of the protolith with only minor features of intracrystalline plastic deformation. It is suggested that the increased IPO of porphyroclasts results from more rigid body rotation of plagioclase within the weaker biotite and quartz matrix during solid-state deformation.

4.2. High strain, lower temperature (sample E–S)

The IPO of the new grains (Fig. 14b) is always weaker than the IPO of the porphyroclasts (Fig. 14a) despite the fact that a much larger number of grains was measured (in the same area of sample). The preferred orientation of $n-\gamma$ is approximately normal to the foliation plane, and $n-\alpha$ forms a maximum close to the stretching lineation. This orientation pattern suggests that the (010)[100] slip system of the recrystallized grains was preferentially in a favourable orientation for slip in the kinematic reference frame of the samples. However, the pattern of the IPO of new grains is similar to that of the protolith phenocrysts, which results from rigid body rotation and not from intracrystalline plasticity. Therefore, the IPO of the new grains cannot be unequivocally interpreted as the result of crystal plastic deformation (see also Shelley (1977, 1986) and Berger and Stünitz (1996) for similar interpretations).

An independent test to constrain the slip system was carried out by measuring the orientation of some bent albite twin planes (010) with the U-stage in order to define the misorientation axis, and thus the slip direction (approximately normal to the misorientation axis and contained in (010) for tilt boundaries) on such twin planes. The direction normal to the misorientation axis (in the albite twin plane) is approximately parallel to $n-\alpha$, which makes an angle of only 15° with [100]. It is therefore suggested that one active slip system was indeed (010)[100]. (010) is the most commonly observed slip plane in experimentally and naturally deformed plagioclase (Marshall and McLaren, 1977; Olsen and Kohlstedt, 1984; Goode, 1978; Montardi and Mainprice, 1987; Ji et al., 1988; Ague et al., 1990; Kruse et al., 2001). The [100] slip direction is unusual (the more frequently observed direction is [001]), but has been inferred by some authors (Kruhl,

Fig. 14. Stereoplots (lower hemisphere) illustrating the IPO of plagioclase grains. Horizontal line: foliation. L: lineation. (A) IPO of the protolith and of the porphyroclasts in sample E–S. Data contoured at 1.0, 2.0, …, 4.0; (B) IPO of the new grains in the high-strain samples E–S, C–S, and W–S. Data contoured at 1.0, 1.5, 2.0, …, 4.5; (C) IPO of a core and mantle structure in sample E–S, in which the orientation of $n\alpha$ and $n\beta$ of the core differ from the maxima of $n\alpha$ and $n\beta$ of the new grains. Porphyroclast orientation is indicated by diamond symbol. Contour intervals at 1.0, 1.5, 2.0, …, 4.0.

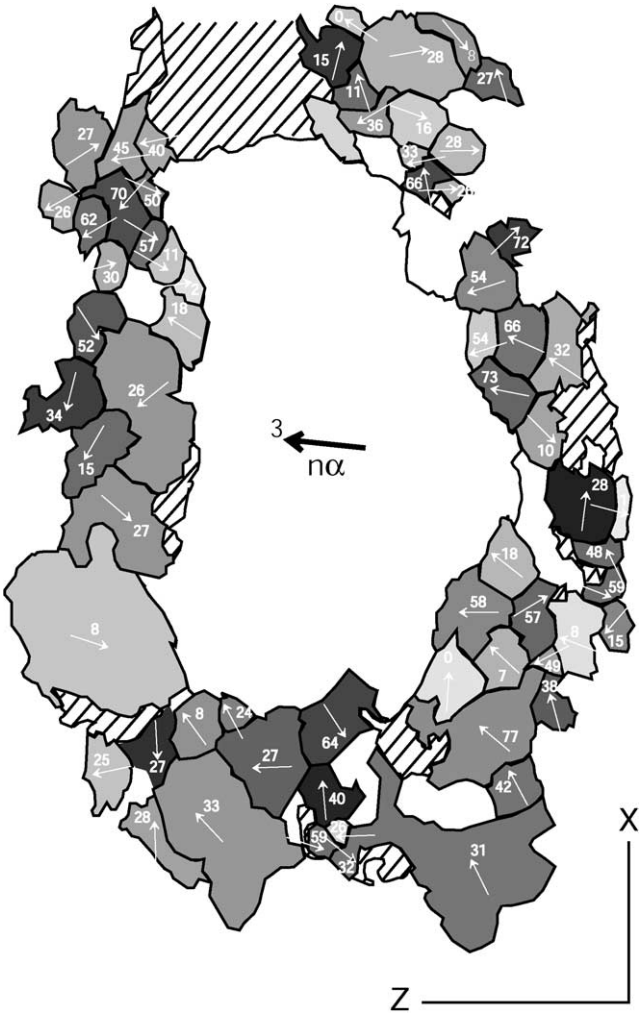

Fig. 15. Distribution of the $n-\alpha$ axis of the optic indicatrix in the new grains forming a mantle around an old grain in sample C–S. The stretching lineation of the sample is oriented vertically (X). The intensity of the grey fillings of the new grains is proportional to the misorientation between new and old grains. White arrows indicate the dip direction of $n-\alpha$, relative to the *XZ* plane. White numbers indicate the dip angle. Open grains: plagioclase grains whose orientation could not be measured on the U-stage. Hatched grains: grains of composition other than plagioclase. No systematic trend in the orientation of $n-\alpha$ from the core to the outer part of the mantle occurs.

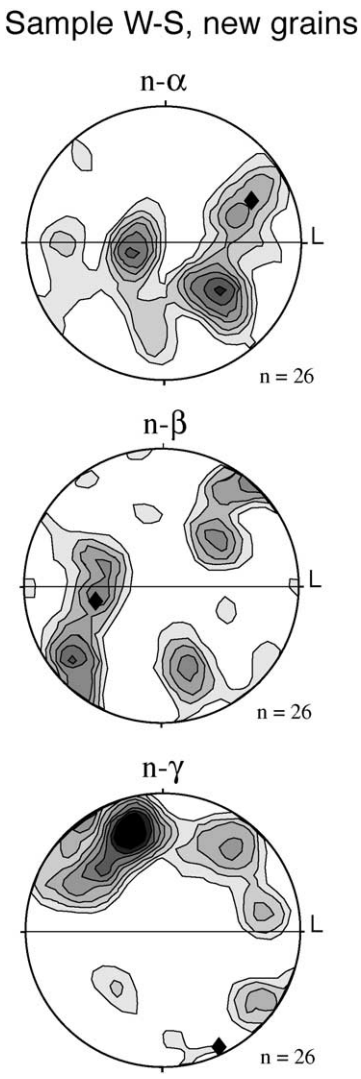

Fig. 16. High T, high strain sample W–S. IPO of new grains from the pressure shadow of a large porphyroclast. The porphyroclast orientation is indicated by a diamond symbol. Contour intervals at 1.0, 1.5, 2.0, …, 5.0. Note the close spatial association of IPO from porphyroclast and new grains.

1987a,b), and it is consistent with the IPO pattern of the new grains (Fig. 14b).

In order to test whether the orientation of the new grains in sample E–S is inherited from the old clasts or is controlled by the active slip system, we selected a core and mantle structure in which the porphyroclast's $n-\alpha$ and $n-\beta$-directions differ from those of the maxima shown for new grains in Fig. 14b. The IPO of the new grains forming the mantle of this porphyroclast (Fig. 14c) shows that $n-\alpha$ is oriented close to the lineation and $n-\beta$ approximately normal to the lineation. In the porphyroclast, $n-\beta$ is almost exactly parallel to the stretching lineation. Thus, the orientation of the new grains does not seem to be inherited from the old grain, in spite of the widespread parallelism between IPOs of old and new grains in pole figures (Fig. 14a and b). Since there is no host control on the orientation of new grains, we infer that progressive subgrain rotation is not the recrystallization mechanism for the formation of new grains. This interpretation is consistent with the results of the chemical analyses of old and new grains (Figs. 2 and 6b) suggesting nucleation and growth of new grains instead of subgrain rotation.

4.3. High strain, intermediate temperature (sample C–S)

The IPO of the new grains (Fig. 14b) exhibits a well defined pattern, with $n-\gamma$ normal to the foliation plane, and $n-\alpha$ approximately parallel to the lineation. This orientation pattern is similar to that of the new grains in sample E–S, and it is also consistent with slip on (010)[100]. The

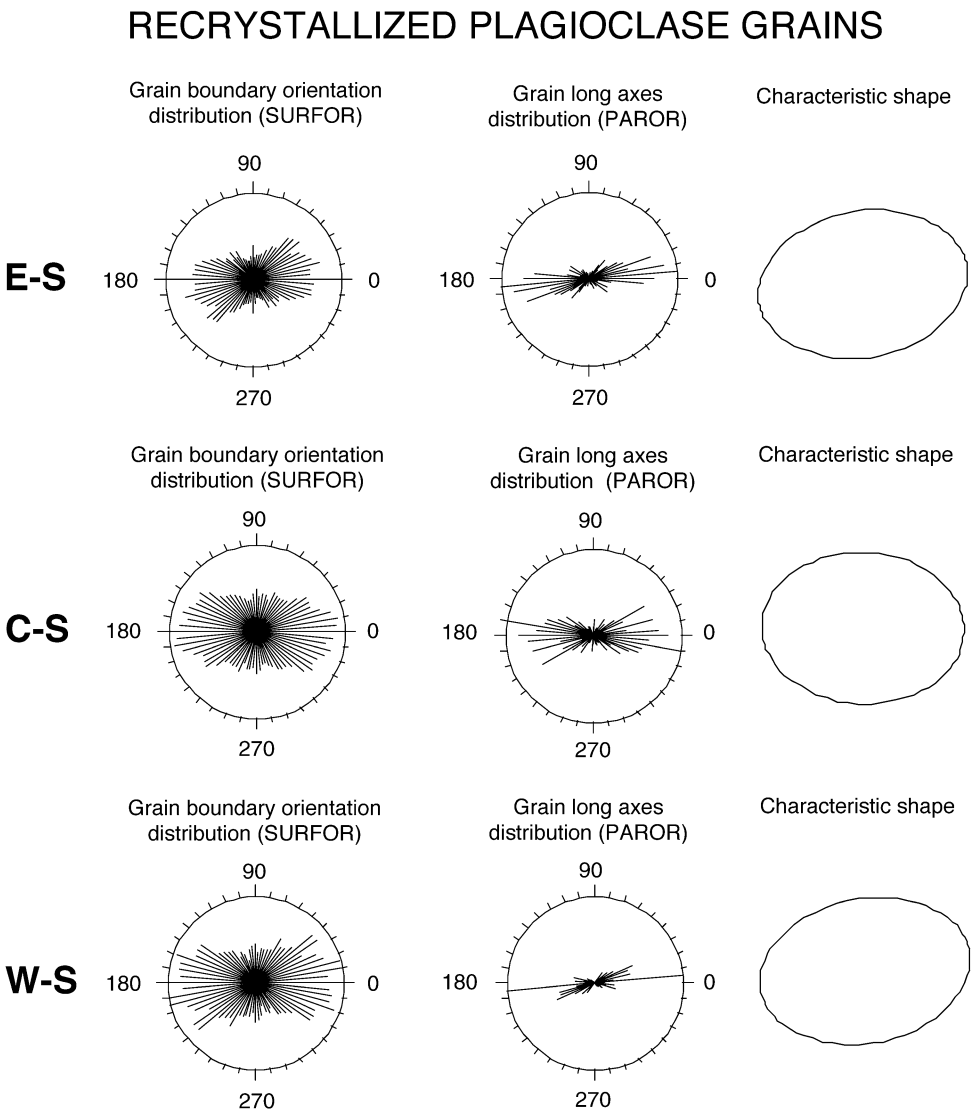

Fig. 17. Image analysis of plagioclase new grains from the high strain samples E–S, C–S, and W–S. Foliation and lineation are horizontal.

IPO of new grains of a core and mantle structure (Fig. 15) shows that most new grains have a high misorientation with respect to the core. Thus, most grains do not show any host control, suggesting that they did not form by progressive subgrain rotation. This interpretation is consistent with the light microscope observations of limited subgrain formation.

4.4. High strain, high temperature (sample W–S)

The IPO of plagioclase new grains in the plagioclase–biotite matrix is more uniform than in other samples, except for a weak girdle distribution of $n-\alpha$ (Fig. 14b). This result is unexpected, because the bulk strain that affected the plagioclase aggregates is much larger in this sample than in the samples C–S and E–S due to increased partitioning of deformation into plagioclase at higher temperature conditions. This increase of strain with increasing temperature is shown by the increase in the aspect ratios of plagioclase aggregates from E to W (Fig. 7; see below also). The weakening of the IPO associated with increasing temperature and strain may be the result of deformation processes in which intracrystalline plasticity only plays a subordinate role. In contrast to the IPO in the plagioclase–biotite matrix (Fig. 14b), the IPO of new grains in the pressure shadow of a plagioclase porphyroclast (where biotite is absent) shows a stronger preferred orientation in spite of the small number of grains measured (Fig. 16). The mixed plagioclase + biotite aggregates have experienced higher strain than the pure plagioclase in the pressure shadow (Fig. 16). Thus, the more strongly deformed matrix domains exhibit a weaker IPO than the lesser deformed pure plagioclase domains. A weak crystallographic preferred orientation during deformation is consistent with a deformation mechanism of grain boundary sliding (Edington et al., 1976; Padmanabhan and Davies, 1980). The pressure shadow domain shows a

host-control relationship between the new grains and porphyroclast, especially for $n-\gamma$ and $n-\beta$ (Fig. 16). The host control indicates that progressive subgrain rotation probably is the dominant recrystallization mechanism, consistent with light microscope observations of subgrains in the porphyroclasts. (Ji and Mainprice, 1990; Kruse et al., 2001, 2002).

5. Image analysis

The microstructures of the newly formed plagioclase grains in the high strain samples were quantitatively investigated using image analysis techniques (PAROR, SURFOR, and SHAPES programs of Panozzo (1983, 1984) and Panozzo and Hürlimann (1983). The program PAROR measures the average orientation of the long axes of grains, and the program SURFOR measures the orientation of the individual segments of grain boundaries. The program SHAPES calculates the ratio of the length of the actual grain boundary versus the length of the outline of the grain projection (the grain projection outline can be envisaged as putting a rubber band around the grain). The resulting value, termed the 'Paris factor' (Panozzo and Hürlimann, 1983), gives an estimate of how lobate the grain boundaries are. A straight line or a circle have a Paris factor of 100% (the smaller the Paris factor, the more lobate the boundaries).

5.1. High strain, lower temperature (sample E–S)

The Paris factor is very high (95.4%), confirming the straight character of the plagioclase grain boundaries. However, the shapes of the grains are not isotropic, as indicated by the distribution of the long axes of the grains and by the distribution of the grain surfaces (Fig. 17), which both indicate a preferred orientation subparallel to the foliation plane. Such an alignment of grains and grain boundaries suggests that these plagioclase aggregates were generated by a syndeformational re- or neocrystallization.

5.2. High strain, intermediate temperature (sample C–S)

The shape anisotropy of the grains is weaker compared with the high strain sample of the Easternmost cross-section (E–S), as shown by the more equant characteristic shape in Fig. 17. In contrast, the shape anisotropy of the aggregates, i.e. the elongate lenses of new grains (Fig. 7) is much higher than in sample E–S. Moreover, compared with sample E–S, grain boundaries are more lobate, as shown by the smaller value of the Paris factor (87.6%). These observations indicate a higher grain boundary mobility compared with sample E–S. This inference is consistent with the interpretation of formation of new grains by subgrain rotation and grain boundary migration.

5.3. High strain, high temperature (sample W–S)

Grain boundaries are generally lobate but can locally be straight. The Paris factor for the plagioclase–plagioclase contacts is 82.6%, indicating that grain boundaries are more lobate than in lower temperature samples. More lobate grain boundaries are consistent with recrystallization by grain boundary migration recrystallization, which becomes more important to the West with increasing temperature producing more lobate grain boundaries.

6. Discussion

The observations described above indicate a progressive change in the microstructure of plagioclase from lower temperature (Eastern cross-section) to higher temperature (Western cross-section). With increasing temperature, the average size of the new grains progressively increases from 120 to 330 to 370 μm, the grain boundaries become increasingly lobate, the IPO becomes increasingly weaker, and the compositional difference between old and new grains becomes increasingly smaller. These observations point to transitions in the recrystallization/neocrystallization and deformation processes of plagioclase over the studied temperature range of deformation, from 580 to 670 °C.

6.1. Recrystallization and neocrystallization

New grains of plagioclase are common in high strain samples of the Eastern low temperature cross-section, but there is no microstructural or crystallographic evidence for subgrain rotation recrystallization. Optical-scale subgrains are lacking, the boundary between the porphyroclast and mantle is sharp, misorientation of new grains does not increase from the inner towards the outer margin of the mantle, there is no host-control of the new grain orientations, and the anorthite content of the new grains in the mantle differs from that of the porphyroclasts by about 20%. Compositional changes of plagioclase grains can result from the migration of one grain into a neighbouring grain of different composition (Hay and Evans, 1987; Yund and Tullis, 1991), whereas recrystallization by progressive subgrain rotation cannot account for a compositional change (Stünitz, 1998). Before boundaries of grains with different composition can migrate, these compositionally different grains have to nucleate first. We therefore suggest that the core and mantle structures in our samples of the Eastern cross-section result from nucleation and growth of new grains along the margins of the porphyroclasts, where dislocation densities and stresses are highest (e.g. Sodre Borges and White, 1980). Thus, the sites of nucleation of new grains are partially controlled by deformation, but the nature of the driving potential for nucleation and growth is largely chemical.

There is only a small amount of evidence for progressive subgrain rotation in plagioclase as the dominant recrystallization mechanism (e.g. Olsen and Kohlstedt, 1985; White and Mawer, 1986; Ji and Mainprice, 1990; Kruse et al., 2001, 2002) in the literature on recrystallization of naturally

deformed plagioclase (Vernon, 1975; White, 1975; Goode, 1978; Brown et al., 1980; Sodre Borges and White, 1980; Jensen and Starkey, 1985; Montardi and Mainprice, 1987; Olesen, 1987; Ji et al., 1988; Ague et al., 1990) and of experimentally deformed plagioclase (Marshall and McLaren, 1977; Tullis and Yund, 1985, 1991; Dell'Angelo and Tullis, 1996; Tullis, 1990). Instead, most recrystallization features of plagioclase are similar to regime 1 recrystallization described for quartz by Hirth and Tullis (1992), probably because the slow volume diffusion in feldspar (Yund and Tullis, 1991) inhibits dislocation climb and hence subgrain formation (Tullis and Yund, 1985).

At the highest temperatures, in the Western cross-section, there is evidence for subgrain rotation in combination with migration of grain boundaries instead of nucleation and growth. In the low-strain samples, migration of the original grain boundaries takes place. We cannot exclude the possibility that some of the subgrain boundaries inferred from optical observations are due to microfracturing (Tullis and Yund 1987), but on the light microscope scale of observation, the bending of the crystal adjacent to a discontinuous change in orientation is continuous and suggests that at least some crystal plastic deformation is associated with the formation of new grain boundaries.

The transition from nucleation and growth of new grains in the East to subgrain rotation and grain boundary migration in the West appears to be controlled by three factors. (1) Higher temperatures in the West probably allow dislocation climb to occur and hence the formation of subgrain boundaries. (2) Higher temperatures also facilitate grain boundary mobility. (3) At higher temperatures, there is a smaller or no compositional difference between new and old grains, and thus a diminishing chemical driving potential for recrystallization. The dominant recrystallization mechanism in the West is grain boundary migration recrystallization (GBM; Guillopé and Poirier, 1979) with minor subgrain rotation.

Considering that the solidus of the Bergell tonalite was reached at approximately 670 °C (Reusser, 1987), GBM in plagioclase occurred at a comparatively low temperature, well below that (1000 °C) noted by Lafrance et al. (1996) for a deformed anorthosite. The reason for activating GBM at low temperatures could be the presence of a small amount of residual melt or H_2O during deformation of plagioclase. In experiments, the presence of small amounts of melt can enhance dynamic recrystallization (e.g. Dell'Angelo and Tullis, 1988; Jin et al., 1994), although the opposite effect has also been observed in basaltic systems (e.g. Hirth and Kohlstedt, 1995), and therefore a conclusive interpretation is not possible yet (see Rosenberg (2001) for discussion).

The microstructural changes associated with increasing temperature described above suggest that the sequence of recrystallization mechanisms in plagioclase differs from that seen in quartz (Hirth and Tullis, 1992), which progresses from bulging recrystallization (regime 1) to rotation recrystallization (regime 2) to grain boundary migration recrystallization (regime 3). The Bergell samples show the transition from recrystallization by nucleation and growth of new grains of different composition at the lowest temperature, to rotation recrystallization associated with grain boundary migration at higher temperature. The chief reason for the different behaviour of quartz and plagioclase is that in the low temperature regime, recrystallization of plagioclase may involve a change in chemical composition.

6.2. Deformation mechanisms

The mechanical behaviour of plagioclase, inferred from microstructures, at low strain changes dramatically from low to high temperature in the investigated range of temperatures. At low temperature ($\geq$580 °C), plagioclase is largely rigid; limited internal deformation occurs mostly by fracturing. Deformation partitions into weaker quartz + biotite layers (Fig. 6). In contrast, at higher temperatures ($\leq$670 °C), there is no evidence that plagioclase is stronger than the other phases in the quartz–biotite–plagioclase matrix (Figs. 12 and 13). For dislocation creep deformation, such a relative change in mechanical strength with increasing temperature could only be explained by higher activation energy for plagioclase compared with the other phases. Although plagioclase activation energies are somewhat higher than in quartz (Luan and Paterson, 1992; Gleason and Tullis, 1995; Hirth et al., 2001; Dimanov and Diesen, 2001; Offeraus et al, 2001), a switch in relative strength between quartz and plagioclase is difficult in the temperature range of 580–670 °C. Thus, the relative strength change of plagioclase with increasing temperature cannot be explained by dislocation creep deformation.

We infer a contribution of diffusion creep (diffusion accommodated grain boundary sliding) to the deformation of the rock in high temperature samples. This inference is, among other criteria, based on the dispersed distribution of biotite throughout the deformed and recrystallized plagioclase aggregates in all high temperature samples. Such a dispersed distribution of biotite and plagioclase is common in high-temperature deformed granitic rocks (e.g. Martelat et al. (1999) for granulite facies rocks and Schulmann et al. (1996) for amphibolite facies tonalites). The dispersion of plagioclase and biotite takes place during deformation, because biotite is a reaction product which forms during solid state deformation (Berger and Stünitz, 1996).

Biotite and plagioclase have very different deformational behaviour under amphibolite facies temperature conditions: biotite is a mechanically weak phase (Kronenberg et al., 1990; Shea and Kronenberg, 1992), whereas plagioclase is quite strong (Tullis, 1983). If crystal plastic deformation is the dominant deformation mechanism, domains of weak phases tend to coalesce to form interconnected weak layers (Jordan, 1986; Handy, 1990; Tullis, 1990). In the Western cross-section, several observations suggest that crystal plasticity is not a dominant deformation mechanism in plagioclase–biotite aggregates: (1) the new biotite grains do not show any coalescence. Plagioclase and biotite are well

dispersed; (2) the IPO of the new plagioclase grains is considerably weaker than that of the starting material (phenocrysts of magmatic rocks and porphyroclasts) and that of pure plagioclase domains deformed to lower strains (Figs. 14 and 16). A weakening of the crystallographic preferred orientation during deformation is consistent with grain boundary sliding deformation (Edington et al., 1976; Padmanabhan and Davies, 1980); (3) grain boundaries tend to be aligned along several grains. Such grain boundary alignments occur during grain boundary sliding in different materials (Drury and Humphreys, 1988).

The dispersion of plagioclase grains among other phases increases from East to West (Fig. 7), together with the strain accommodated by plagioclase-dominated domains. Thus, the higher dispersion of plagioclase correlates with an increase in finite strain.

Deformation of the Bergell tonalite took place during retrograde metamorphism, whereby biotite grew at the expense of hornblende (Berger and Stünitz, 1996). Local pressure gradients develop during grain boundary sliding (Poirier, 1985), providing low pressure sites for the precipitation of biotite grains between new grains of plagioclase. A similar process for the nucleation of hornblende between plagioclase grains has been inferred by Kruse and Stünitz (1999) for anorthosites deformed at amphibolite facies conditions, where deformation also involved grain boundary sliding. Thus, deformation by diffusion-accommodated grain boundary sliding is a likely mechanism that may explain the microstructures of dispersed phases and the IPO of the plagioclase in the high temperature tonalite samples.

7. Conclusions

The present study shows that the deformation processes and recrystallization mechanisms of plagioclase in the amphibolite facies are strongly influenced by relatively small temperature changes, within the range 580–670 °C. At low strain, there is a transition from mostly fracturing at the lowest temperatures to dislocation creep at intermediate temperatures. Syndeformational recrystallization at intermediate temperatures involves progressive subgrain rotation with some local grain boundary migration. At higher strain, compositional disequilibrium is probably the main driving potential for plagioclase recrystallisation at lower temperatures, whereas at higher temperatures, the chemical driving potential for recrystallization decreases, and the recrystallization becomes driven by internal strain energy. At the highest temperatures, recrystallization takes place by grain boundary migration recrystallization. The transition to dominant grain boundary migration is associated with a pronounced increase in the volume proportion of recrystallized grains.

We infer that the dominant deformation mechanism at the highest temperatures (≤670 °C) is not intracrystalline plasticity but diffusion accommodated grain boundary sliding in a phase mixture of plagioclase and biotite. Intracrystalline plasticity continues to be an active process of deformation and is important for the formation of new grains, but it does not accommodate the high strain of the samples at the highest temperatures.

The present study suggests that rheological data obtained for crystal plastic dislocation creep of monomineralic plagioclase might not adequately represent the rheological behaviour of an amphibolite facies middle to lower crust. Applying only dislocation creep flow laws for feldspar tends to overestimate the strength of the crust. Constitutive relationships for polyphase rocks (certainly if they contain plagioclase) should consider and incorporate diffusion creep deformation processes.

Acknowledgements

During this study, numerous discussions with A. Berger, R. Heilbronner, St. Schmid, C. Davidson and B. John have helped us to understand many aspects of the deformation of plagioclase. The manuscript has benefited greatly from the very constructive and thorough reviews by J. Tullis and A. Post. Financial support by the Schweizerischer Nationalfonds n. 20-35891.92 is gratefully acknowledged.

References

Ague, D.M., Wenk, H.R., Wenk, E., 1990. Deformation microstructures and lattice orientations of plagioclase in gabbros from Central Australia. Geophysical Monograph 56, 173–186.

Berger, A., Stünitz, A., 1996. Deformation mechanisms and reaction of hornblende: examples from the Bergell tonalite. Tectonophysics 257, 149–174.

Berger, A., Rosenberg, C.L., Schmid, S.M., 1996. Ascent, emplacement and exhumation of the Bergell pluton within the Southern Steep Belt of the Central Alps. Schweizerische Mineralogische und Petrographische Mitteilungen 76, 357–382.

Brodie, K., 1981. Variation in amphibole and plagioclase composition with deformation. Tectonophysics 78, 385–402.

Brown, W.L., Macaudière, J., Ohnenstetter, M., 1980. Ductile shear zones in a meta-anorthosite from Harris, Scotland: textural and compositional changes in plagioclase. Journal of Structural Geology 2, 281–287.

Burri, C., Parker, R.L., Wenk, E., 1967. Die optische Bestimmung der Plagioklase. Birkhäuser, Basel.

Davidson, C., Rosenberg, C.L., Schmid, S.M., 1996. Synmagmatic folding of the base of the Bergell pluton: evidence from the western contact. Tectonophysics 265, 213–238.

Dell'Angelo, L.N., Tullis, J., 1988. Experimental deformation of partially melted granitic aggregates. Journal of Metamorphic Geology 6, 495–515.

Dell'Angelo, L.N., Tullis, J., 1996. Textural and mechanical evolution with progressive strain in experimentally deformed aplite. Tectonophysics 256, 57–82.

Dimanov, A., Dresen, G., 2001. Rheology of fine grained anorthite-diopside aggregates. Abstract International Conference DRT, Utrecht, p. 43.

Drury, M.R., Humphreys, F.J., 1988. Microstructural shear criteria associated with grain-boundary sliding during ductile deformation. Journal of Structural Geology 10, 83–89.

Edington, J.W., Melton, K.N., Cutler, C.P., 1976. Superplasticity. Progr. Material Science 21, 61–170.

Fisch, H.R., 1989. Zur Kinematik der südlichen Steilzone der Zentralalpen, E von Bellinzona. Schweizerische Mineralogische und Petrographische Mitteilungen 69, 377–393.

Fitz Gerald, J.D., Stünitz, H., 1993. Deformation of granitoids at low metamorphic grade. I: reactions and grain size reduction. Tectonophysics 221, 269–297.

Fumasoli, M.W., 1974. Geologie des Gebietes nördlich und südlich der Iorio–Tonale–Linie im Westen von Gravedona. PhD thesis, Universitat Zurich.

Gleason, G.C., Tullis, J., 1995. A flow law for dislocation creep of quartz aggregates determined with the molten salt cell. Tectonophysics 247, 1–23.

Goode, A.D.T., 1978. High temperature, high strain rate deformation in the lower Kalka Intrusion, central Australia. Contributions to Mineralogy and Petrology 66, 137–148.

Gower, R.J.W., Simpson, C., 1992. Phase boundary mobility in naturally deformed, high-grade quartzofeldspathic rocks: evidence for diffusional creep. Journal of Structural Geology 14, 301–313.

Guillopé, M., Poirier, J.P., 1979. Dynamic recrystallization during creep of single-crystalline halite: an experimental study. Journal of Geophysical Research 84, 5557–5567.

Handy, M., 1990. The solid state flow of polymineralic rocks. Journal of Geophysical Research, 95, 8647–8661.

Hay, R.S., Evans, B., 1987. Chemically induced grain boundary migration in calcite: temperature dependence, phenomenology, and possible applications to geologic systems. Contributions to Mineralogy and Petrology 97, 127–141.

Heitzmann, P., 1987. Evidence of late Oligocene–early Miocene backthrusting in the Central Alpine "root zone". Geodinamica Acta 1, 183–192.

Hirth, G., Tullis, J., 1992. Dislocation creep regimes in quartz aggregates. Journal of Structural Geology 14, 145–159.

Hirth, G., Kohlstedt, D.L., 1995. Experimental constraints on the dynamics of the partially molten upper mantle 2. Deformation in the dislocation creep regime. Journal of Geophysical Research 100, 15441–15449.

Hirth, G., Teyssier, C., Dunlap, W.J., 2001. An evaluation of quartzite flow laws based on comparisons between experimentally and naturally deformed rocks. International Journal of Earth Sciences (Geologische Rundschau) 90, 77–87.

Hobbs, B.E., 1968. Recrystallization of single crystals of quartz. Tectonophysics, 6, 353–401.

Jensen, L.N., Starkey, J., 1985. Plagioclase microfabrics in a ductile shear zone from the Jotun Nappe, Norway. Journal of Structural Geology 7, 527–539.

Ji, S., Mainprice, D., 1990. Recrystallization and fabric development in plagioclase. Journal of Geology 98, 65–79.

Ji, S., Mainprice, D., Boudier, F., 1988. Sense of shear in high-temperature movement zones from the fabric asymmetry of plagioclase feldspars. Journal of Structural Geology 10, 73–81.

Jin, Z., Green, H.W., Zhou, Y., 1994. Melt topology in partially molten mantle peridotite during ductile deformation. Nature 372, 164–167.

Jordan, P.J., 1987. The deformational behaviour of bimineralic limestone–halite aggregates. Tectonophysics, 135, 185–197.

Kronenberg, A.K., Kirby, S.H., Pinkston, J., 1990. Basal slip and mechanical anisotropy of biotite. Journal of Geophysical Research 95, 19257–19279.

Kruhl, J.H., 1987a. Preferred lattice orientations of plagioclase from amphibolite and greenschist facies rocks near the Insubric Line (Western Alps). Tectonophysics 135, 233–242.

Kruhl, J.H., 1987b. Zur Deformation und Gitterregelung des Plagioklases. Jahrbuch der Geologische Bundesanstalt 130, 205–243.

Kruse, R., Stünitz, H., 1999. Deformation mechanisms and phase distribution in mafic high-temperature mylonites from the Jotun Nappe, southern Norway. Tectonophysics 303, 223–249.

Kruse, R, Stünitz, H., Kunze, K., 2001. Dynamic recrystallization processes in plagioclase porphyroclasts. Journal of Structural Geology, 23, 1781–1802.

Kruse, R, Stünitz, H., Kunze, K., 2002. Erratum to "Dynamic recrystallization processes in plagioclase porphyroclasts". [Journal of Structural Geology, 23, 1781–1802]. Journal of Structural Geology, 24, 587–589.

Lafrance, B., John, B.E., Scoates, J.S., 1996. Synemplacement recrystallization and deformation microstructures in the Poe Mountain anorthosite, Wyoming. Contributions to Mineralogy and Petrology 122, 431–440.

Luan, F.C., Paterson, M.S., 1992. Preparation and deformation of synthetic aggregates of quartz. Journal of Geophysical Research 97, 301–320.

Marshall, D.B., Vernon, R.H., Hobbs, B.E., 1976. Experimental deformation and recrystallization of a peristerite. Contributions to Mineralogy and Petrology 57, 49–54.

Marshall, D.B., Mclaren, A.C., 1977. Deformation mechanisms in experimentally deformed plagioclase feldspars. Physics and chemistry of minerals, 1, 351–370.

Martelat, J.-E., Schulmann, K., Lardeaux, J.-M., Nicollet, C., Cardon, H., 1999. Granulite microfabrics and deformation mechanisms in southern Madagascar. Journal of Structural Geology 21, 671–688.

Molli, G., 1994. Microstructural features of high temperature shear zones in gabbros of the Northern Appennine Ophiolites. Journal of Structural Geology 16, 1535–1541.

Montardi, Y., Mainprice, D., 1987. A transmission electron microscopic study of the natural plastic deformation of calcic plagioclases (An 68–70). Bulletin Mineralogique 110, 1–14.

Offeraus, L.J., Wirth, R., Dresden, G., 2001. Triaxial high-temperature creep of polycrystalline albite. Abstract International Conference DRT, Utrecht, p. 124.

Olesen, N.Ø., 1987. Plagioclase fabric development in a high-grade shear zone, Jotunheimen, Norway. Tectonophysics 142, 291–308.

Olsen, T.S., Kohlstedt, D.T., 1984. Analysis of dislocations in some naturally deformed plagioclase feldspars. Physics and Chemistry of Minerals 11, 153–160.

Olsen, T.S., Kohlstedt, D.T., 1985. Natural deformation and recrystallization of some intermediate plagioclase feldspars. Tectonophysics 111, 107–131.

Ord, A., Hobbs, B.E., 1989. The strength of the continental crust, detachment zones and the development of plastic instabilities. Tectonophysics 158, 269–289.

Padmanabhan, K.A., Davies, G.J., 1980. Superplasticity. Materials Research and Engineering. Springer, Berlin.

Panozzo, R., 1983. Two-dimensional analysis of shape fabric using projections of lines in a plane. Tectonophysics 95, 279–294.

Panozzo, R., 1984. Two dimensional strain from the orientation of lines in a plane. Journal of Structural Geology 6, 215–221.

Panozzo, R., Hürlimann, H., 1983. A simple method for the quantitative discrimination of convex and convex–concave lines. Microscopica Acta 87, 169–176.

Poirier, J.P., 1985. Creep of Crystals. High-temperature Deformation Processes in Metals, Ceramics and Minerals. Cambridge University Press, p. 260.

Reusser, E., 1987. Phasenbeziehungen im Tonalit der Bergeller Intrusion. PhD, ETH Zurich.

Rosenberg, C.L., 1996. Magmatic and solid state flow during the emplacement of the western bergell Pluton: field studies and microstructural analysis. PhD thesis, University of Basel.

Rosenberg, C.L., 2001. Deformation of partially-molten granite: a review and comparison of experimental and field investigations. International Journal of Earth Sciences (Geologische Rundschau) 90, 60–76.

Rosenberg, C., Heller, F., 1997. Tilting of the Bergell pluton and Central Leopontine area: combined evidence from paleomagnetic, structural and petrological data. Eclogae Geologicae Helvetiae 90, 345–356.

Rosenberg, C., Berger, A., Heilbronner, R., 1994. Deformation of polyphase rocks at different temperature conditions (I): rheological versus mineralogical phases in the Bergell tonalite. Annales Geophysicae 12 (Abstract).

Rosenberg, C., Berger, A., Schmid, S.M., 1995. Observations from the floor of a granitoid pluton: inferences on the driving force of final emplacement. Geology 23, 443–446.

Schmid, S.M., Aebli, H.R., Heller, F., Zingg, A., 1989. The role of the Periadriatic Line in the tectonic evolution of the Alps. In: Coward, M.P., Dietrich, D. (Eds.), Alpine Tectonics. Geological Society Special Publication 45, pp. 153–171.

Schulmann, K., Mlcoch, B., Melka, R., 1996. High-temperature microstructures and rheology of deformed granite, Erzgebirge, Bohemian Massif. Journal of Structural Geology 18, 719–734.

Schmid, S.M., Zingg, A., Handy, M., 1987. The kinematics of movement along the Insurbric Line and the emplacement of the Ivrea Zone. Tectonophysics, 35, 47–66.

Selverstone, J., 1993. Micro- to macroscale interactions between deformational and metamorphic processes, Tauern Window, eastern Alps. Schweizerische Mineralogische und Petrographische Mitteilungen, 73, 229–239.

Shea, W.T., Kronenberg, A.K., 1992. Rheology and deformation mechanisms of an isotropic mica schist. Journal of Geophysical Research 97, 15201–15237.

Shelley, D., 1977. Plagioclase preferred orientation in Haast Schist, NZ. Journal of Geology 85, 65–75.

Shelley, D., 1986. Natural deformation and recrystallization of some intermediate plagioclase feldspars—a discussion on preferred orientation development. Tectonophysics 124, 359–364.

Sodre Borges, F., White, S.H., 1980. Microstructural and chemical studies of sheared anorthosites, Roneval, South Harris. Journal of Structural Geology 2, 273–280.

Stünitz, H., 1998. Syndeformational recrystallization—dynamic or compositionally induced? Contributions to Mineralogy and Petrology 131, 219–236.

Trommsdorff, V., Nievergelt, P., 1983. The Bregaglia (Bergell) Iorio Intrusive and its field relations. Memorie della Societa Geologica Italiana 26, 55–68.

Trümpy, R., 1980. Geology of Switzerland, Part A. Schweizerische Geologische Kommission, Wepf & Co. Publishers, Basel, New York.

Tullis, J., 1983. Deformation of feldspars. In: Ribbe, P.H. (Ed.), Feldspar Mineralogy. Reviews in Mineralogy 2, pp. 297–322.

Tullis, J., 1990. Experimental studies of deformation mechanisms and microstructures in quartzo-feldspathic rocks. In: Barber, D.J., Meredith, P.G. (Eds.). Deformation Processes in Minerals, Ceramics and Rocks. Unwyn Hyman, London, pp. 190–227.

Tullis, J., Yund, R.A., 1985. Dynamic recrystallization of feldspar: a mechanism for ductile shear zone formation. Geology 13, 238–241.

Tullis, J., Yund, R.A., 1987. Transition from cataclastic flow to dislocation creep of feldspar: mechanisms and microstructures. Geology 15, 606–609.

Tullis, J., Yund, R.A., 1991. Diffusion creep in feldspar aggregates: experimental evidence. Journal of Structural Geology 13, 987–1000.

Tullis, J., Yund, D., Farver, J., 1996. Deformation-enhanced fluid distribution in feldspar aggregates and implications for ductile shear zones. Geology 24, 63–66.

Vernon, R.H., 1975. Deformation and recrystallization of a plagioclase grain. The American Mineralogist 60, 884–888.

Villa, I., von Blankenburg, F., 1991. A hornblende Ar–Ar age traverse of the Bregaglia tonalite (SE Central Alps). Schweizerische Mineralogische und Petrographische Mitteilungen 71, 73–87.

Vogler, S., Voll, G., 1976. Fabrics and metamorphism from tonalite, granitic augengneiss and Tonale Series at the S-margin of the Swiss Alps, E of Bellinzona. Schweizerische Mineralogische und Petrographische Mitteilungen 56, 635–640.

Vogler, S., Voll, G., 1981. Deformation and metamorphism at the southmargin of the Alps, East of Bellinzona. Geologische Rundschau 70, 1232–1262.

Watts, M.J., Williams, G.D., 1983. Strain geometry, microstructure and mineral chemistry in metagabbro shear zones: a study of softening mechanisms during progressive mylonitization. Journal of Structural Geology 5, 507–517.

White, J.C., Mawer, C.K., 1986. Extreme ductility of feldspars from a mylonite, Parry Sound, Canada. Journal of Structural Geology 8, 133–143.

White, S., 1975. Tectonic deformation and recrystallization of oligoclase. Contributions to Mineralogy and Petrology 50, 287–304.

White, S., 1976. The effects of strain on the microstructures, fabrics, and deformation mechanisms in quartzites. Philosophical Transactions of the Royal Society of London A 283, 69–86.

Yund, R.A., Tullis, J., 1991. Compositional changes of minerals associated with dynamic recrystallization. Contributions to Mineralogy and Petrology 108, 335–346.